Published OnlineFirst January 18, 2011; DOI: 10.1158/0008-5472.CAN-10-2274

Dual IGF-I/II–Neutralizing Antibody MEDI-573 Potently Inhibits IGF Signaling and Tumor Growth

Jin Gao[1], Jon W. Chesebrough[1], Susan A. Cartlidge[2], Sally-Ann Ricketts[2], Leonard Incognito[1], Margaret Veldman-Jones[2], David C. Blakey[2], Mohammad Tabrizi[3,4], Bahija Jallal[1], Pamela A. Trail[1], Steven Coats[1], Klaus Bosslet[1], and Yong S. Chang[1]

Abstract

Insulin-like growth factors (IGF), IGF-I and IGF-II, are small polypeptides involved in regulating cell proliferation, survival, differentiation, and transformation. IGF activities are mediated through binding and activation of IGF-1R or insulin receptor isoform A (IR-A). The role of the IGF-1R pathway in promoting tumor growth and survival is well documented. Overexpression of IGF-II and IR-A is reported in multiple types of cancer and is proposed as a potential mechanism for cancer cells to develop resistance to IGF-1R–targeting therapy. MEDI-573 is a fully human antibody that neutralizes both IGF-I and IGF-II and inhibits IGF signaling through both the IGF-1R and IR-A pathways. Here, we show that MEDI-573 blocks the binding of IGF-I and IGF-II to IGF-1R or IR-A, leading to the inhibition of IGF-induced signaling pathways and cell proliferation. MEDI-573 significantly inhibited the *in vivo* growth of IGF-I– or IGF-II–driven tumors. Pharmacodynamic analysis demonstrated inhibition of IGF-1R phosphorylation in tumors in mice dosed with MEDI-573, indicating that the antitumor activity is mediated via inhibition of IGF-1R signaling pathways. Finally, MEDI-573 significantly decreased ^{18}F-fluorodeoxyglucose (^{18}F-FDG) uptake in IGF-driven tumor models, highlighting the potential utility of ^{18}F-FDG-PET as a noninvasive pharmacodynamic readout for evaluating the use of MEDI-573 in the clinic. Taken together, these results demonstrate that the inhibition of IGF-I and IGF-II ligands by MEDI-573 results in potent antitumor activity and offers an effective approach to selectively target both the IGF-1R and IR-A signaling pathways. *Cancer Res; 71(3); 1–11. ©2011 AACR.*

Introduction

Insulin-like growth factors (IGF), IGF-I and IGF-II, are small polypeptides involved in regulating cell proliferation, survival, differentiation, and transformation (1–4). They bind to the IGF-I receptor tyrosine kinase (IGF-1R) and insulin receptor isoform A (IR-A; refs. 5, 6) to activate multiple intracellular signaling cascades, including the insulin receptor substrate (IRS) proteins (7), the Akt and MAPK (mitogen-activated protein kinase) pathways (8). IGF-II binds IR-A, a truncated version of the insulin receptor that lacks exon 11, with greater affinity than IGF-I (9). Activation of IR-A by IGF-II results in mitogenic effects and increased survival and motility of tumor cells (10). In contrast, activation of insulin receptors by insulin results primarily in metabolic effects (6, 9, 10). Increased expression of IGF-II or IR-A occurs during fetal development and in certain types of cancers including breast, colorectal, thyroid, bladder, hepatocellular carcinoma, and osteosarcoma (5, 11–18). The overexpression of IR-A and IGF-II may be a potential mechanism leading to resistance to IGF-1R–directed therapies (19, 20). Studies show that downregulation of IGF-1R expression or inhibition of signaling leads to the inhibition of tumor growth (4, 21, 22) and increases the susceptibility of tumor cells to chemotherapeutic agents *in vivo* (3, 4, 8, 23). Both IR-A and IGF-1R are involved in IGF signaling and play significant roles in cancer development and progression (24); therefore, inhibition of both the IR-A and IGF-1R receptors may be required to achieve optimal therapeutic efficacy against IGF-driven cancers (21).

A variety of therapeutic strategies have been evaluated to inhibit the IGF-1R signaling pathway. Monoclonal antibodies that target IGF-1R have shown benefit in early-stage clinical trials (25–27). These antibodies bind to IGF-1R and inhibit IGF binding and signaling. Many of these antibodies induce IGF-1R degradation. A few IGF-1R–specific antibodies can also partially affect the IR-A signaling pathway by targeting IGF-1R/IR-A hybrid receptors (28, 29). However, they do not inhibit IGF-II activation of IR-A homodimers.

Small-molecule IGF-1R kinase inhibitors inhibit IGF-1R, IR-A, and IR-B, due to the highly homologous kinase domains of

Authors' Affiliations: [1]MedImmune, Gaithersburg, Maryland; [2]AstraZeneca Pharmaceuticals, Alderley Park, Macclesfield, United Kingdom; [3]MedImmune, Hayward, California; and [4]AnaptysBio, Inc., San Diego, California

Note: Supplementary data for this article are available at Cancer Research Online (http://cancerres.aacrjournals.org/).

Corresponding Author: Jin Gao, One MedImmune Way, Gaithersburg, MD 20878. Phone: 301-398-5406; Fax: 301-398-8406. E-mail: gaoj@medimmune.com

doi: 10.1158/0008-5472.CAN-10-2274

Published OnlineFirst January 18, 2011; DOI: 10.1158/0008-5472.CAN-10-2274

these receptors (19, 30, 31). The inhibition of IR-B can modulate glucose metabolism *in vivo* resulting in hyperglycemia (26).

We describe the development of a fully human monoclonal antibody, MEDI-573, that neutralizes both the IGF-I and IGF-II ligands and inhibits both IGF-1R and IR-A signaling without affecting the insulin activation of IR. Results from *in vitro* binding, receptor inhibition, and cell growth inhibition studies, as well as tumor xenograft studies, demonstrate the potential therapeutic advantage of targeting both the IGF-1R and the IR-A signaling pathways.

Material and Methods

Antibody generation

MEDI-573 is a fully human IgG2λ monoclonal antibody generated by XenoMouse (Abgenix) technology. MEDI-573 was isolated from mice immunized alternately with soluble recombinant human IGF-I and IGF-II coupled to keyhole limpet hemocyanin. Hybridoma supernatants were screened for binding to IGF-I and IGF-II and the lack of cross-reactivity to human insulin.

Cell lines

The following are mouse embryonic fibroblast (MEF) cell lines that ectopically overexpress specific human proteins: P12 (IGF-1R, IGF-I), C32 (IGF-1R, IGF-II); NIH/IGF-1R (IGF-1R; ref. 32). R-/IRA C9 was a MEF derived from an IGF-1R knockout mouse (33) that ectopically overexpresses human IR-A (9). These cell lines were developed by Dr. Renato Baserga (Thomas Jefferson University) and maintained in Dulbecco's modified Eagle medium (DMEM) supplemented with 10% FBS and different antibiotic supplements: 150 μg/mL hygromycin and 250 μg/mL G418 for P12, 250 μg/mL hygromycin and 750 μg/mL G418 for C32, and 2.5 μg/mL puromycin for R-/IRA C9. Human cancer cell lines (Table 2 and Supplementary Tables 1 and 2) used in the studies were cultured in DMEM with 10% FBS.

BIAcore analysis

Binding affinity of human IGF-I and IGF-II for MEDI-573 was determined by high-resolution surface plasmon resonance using a BIAcore 2000 system. MEDI-573 was immobilized onto a CM5 sensor chip using standard amine coupling to interact with recombinant human IGF-I and IGF-II (R&D Systems). Binding kinetics was analyzed to derive binding affinities. Raw binding data was corrected in the manner described by Myszka (34).

Meso-scale discovery assays

Cells were seeded into tissue culture–treated, 96-well plates in serum-free medium. The next day, cells were treated with IGF-I or IGF-II (Cell Sciences; at 75 ng/mL = 10 nmol/L) or insulin (Sigma; at 58 ng/mL = 10 nmol/L) pre-mixed with serially diluted MEDI-573 or an IGF-1R–specific antibody (produced in-house according to the published sequence of CP-751,871). An IgG2 isotype control antibody was used at 5 and 150 μg/mL. Cells were treated for 15 minutes at 37°C, before being lysed with 50 μL per well lysis buffer (meso-scale discovery, MSD) containing phosphatase inhibitors (Sigma) and protease inhibitors (Roche). The levels of total and phosphorylated IR, IGF-1R, and IRS-1 protein in the lysate were determined using the Insulin Signaling Panel (total protein) and Insulin Signaling Panel (phosphoproteins) Whole Cell Lysate kits according to manufacturer's (MSD) protocol. The levels of total and phosphorylated Akt were determined using the Phospho (Ser473)/Total Akt Whole Cell Lysate kit according to manufacturer's (MSD) protocol.

Immunoblotting

Cells were seeded in 6-well plates and treated as described in the previous paragraph. Whole cell extract was prepared in lysis buffer (Cell Signaling Technology) containing phosphatase inhibitors and protease inhibitors. SDS-PAGE of the lysates was performed using pre-cast 4–12% Bis-Tris Gel (Invitrogen). Separated proteins were transferred to nitrocellulose membranes and probed with antibodies specific for pIGF-1R (Cell Signaling Technology), IGF-1R (Santa Cruz), pAkt (Cell Signaling Technology), Akt (Cell Signaling Technology), pErk1/2 (Cell Signaling Technology), Erk1/2 (Cell Signaling Technology), and β-actin (Sigma), followed by HRP (horseradish peroxidase)-conjugated species specific secondary antibodies.

Cell proliferation assays

NIH/IGF-1R cells, R-/IRA C9 cells, or the mixture of these 2 cell lines were seeded into tissue culture–treated, 96-well plates in medium containing 0.1% charcoal-stripped FBS (CS-FBS; Gibco). The next day, cells were treated with MEDI-573, or an IGF-1R–specific antibody, or an IgG2 isotype control antibody, each serially diluted to required concentrations. Thirty minutes later, either IGF-I (20 ng/mL) or IGF-II (40 ng/mL) was added. The concentration of IGF-I and IGF-II used were determined in similar assays to be optimal to stimulate cell proliferation (Supplementary Fig. 3). The numbers of viable cells in each well were determined using Cell Titer Glo (Promega) 3 days later according to manufacturer's protocol.

Relative abundance of IR-A and IR-B expressed in cancer cells

IR-A versus IR-B relative abundance could not be determined at the protein level due to strong sequence similarity (only 12-amino acid difference) and the lack of commercial antibodies specific for the isoforms. The relative abundance of these 2 isoforms was measured at mRNA levels by reverse transcriptase (RT)-PCR as published previously by Sciacca and colleagues (5).

In vivo tumor growth inhibition studies

Tumor xenografts were established by subcutaneous (s.c.) implantation of 5×10^6 P12 or C32 cells into 5- to 6-week-old female athymic (nu/nu) mice (Harlan Sprague Dawley). Mice were randomized into groups of 10 when tumors were 100 to 200 mm^3. MEDI-573 was administered by intraperitoneal (i.p.) injection at indicated dose levels twice per week, for 2 weeks. Tumor volume (mm^3) was measured 2 to 3 times per week and was calculated by: [length (mm) × width $(mm)^2$]/2. Body

Published OnlineFirst January 18, 2011; DOI: 10.1158/0008-5472.CAN-10-2274

weights were measured twice per week. Tumor growth inhibition (TGI) was calculated as $(1 - T/C) \times 100$, where T = final tumor volumes from a treated group, and C = final tumor volumes from the control group. At the end of the studies, mice were administered one last dose of MEDI-573, tumors were harvested 24 or 72 hours later and snap frozen. MedImmune is an AAALAC International-accredited facility.

Evaluation of phosphorylated IGF-1R (pIGF-1R) levels in tumor extracts

Tumor extracts were prepared in Tris-lysis buffer (MSD) supplemented with phosphatase inhibitors and protease inhibitors using a FastPrep-24 homogenizer (MP Biomedical). The total protein concentration of the tumor extract was determined using the BCA (bicinchoninic acid) assay. The levels of total or phosphorylated IGF-1R in the extract were determined using MSD assays as described earlier. The pIGF-1R signals were normalized to the total IGF-1R signals and plotted on Y axis as percent of untreated control against treatment groups on X axis.

^{18}F-FDG-PET imaging

Mice with P12 tumors were randomized into 4 groups of 8 each, 2 vehicle and 2 MEDI-573 groups for readout to be taken 1 day (day 2) or 3 days (day 4) after one dose of treatment. Baseline imaging was carried out on day 0 for all mice. On day 1, mice received either vehicle or MEDI-573 (40 mg/kg i.p.). On day 2 or 4, ^{18}F-FDG-PET imaging was performed for 1 group of the vehicle- or MEDI-573–treated mice. Food was withdrawn at least 4 hours prior to injection of ^{18}F-FDG. Mice were anesthetized and ^{18}F-FDG administered by intravenous (i.v.) injection (mean dose injected was 12.3 MBq per mouse). Mice remained anesthetized during a 45-minute uptake period followed by a 20-minute PET scan using Siemens Inveon PET scanner, followed by 3D (3-dimensional) histogramming and MAP reconstruction. Six animals per group were used for final result analyses.

Image analysis was carried out using Inveon Research Workplace (IRW) software. Standard uptake value (SUV) was calculated using the standard formula as described by Gambhir (35), with maximum SUV (MaxSUV) calculated for each tumor.

Statistics

All samples were analyzed as duplicates, and values are presented as mean ± SEM, unless otherwise specified.

Results

Characterization of MEDI-573, a fully human antibody to human IGF-I and IGF-II

The properties of MEDI-573 are summarized in Table 1. The binding affinity for human IGF-I, IGF-II, or human insulin was determined by BIAcore analysis. No binding was detected against human insulin. Epitope mapping studies indicated that MEDI-573 binds to the epitope that overlaps with F23 and F25 (Supplementary Fig. 1), which are conserved amino acids in both IGF-I and IGF-II essential for binding to IGF-1R (36). F23 (F26 in IGF-II) is also reported to be essential for high-affinity binding to IGF-binding proteins (IGFBP; ref. 37).

MEDI-573 inhibits the IGF-induced activation of IGF-1R

MEDI-573 inhibited the binding of human IGF-I or IGF-II to human IGF-1R and the binding of IGF-II to IR-A protein in ELISA (Supplementary Fig. 2). MSD assays (Fig. 1A and B) show that MEDI-573 inhibited IGF-I–induced (75 ng/mL; A) or IGF-II–induced (75 ng/mL; B) phosphorylation of IGF-1R (IC_{50} = 0.97 and 0.2 μg/mL, respectively), and the downstream signaling proteins IRS-1 (IC_{50} = 1.3 and 0.2 μg/mL, respectively) and Akt (IC_{50} = 4.5 and 0.2 μg/mL, respectively), in NIH/IGF-1R cells (MEF overexpressing human IGF-1R). Immunoblottings (Fig. 1C) show that from 1.5 to 150 μg/mL, MEDI-573 inhibited the IGF-I–induced phosphorylation of IGF-1R, Akt, and Erk1/2, in a dose-dependent manner, without changing the levels of total proteins. Similar results were observed with a number of different IGF-1R–expressing cell lines (Supplementary Table 1). In addition, MEDI-573 inhibited the phosphorylation of IR-A induced by 10 nmol/L of IGF-II, but not 10 nmol/L of human insulin (Fig. 1D), in R-/IRA C9 cells, a mouse IGF-1R knockout MEF cell line overexpressing recombinant human IR-A. This is consistent with the results from BIAcore binding studies (Table 1; raw data not shown) that MEDI-573 does not bind to human insulin.

IGF-I at 20 ng/mL or IGF-II at 40 ng/mL maximally stimulated the *in vitro* proliferation of NIH/IGF-1R cells (Supplementary Fig. 3), which was in turn inhibited by MEDI-573 (IC_{50} = 2.9 and 0.35 μg/mL, respectively; Supplementary Fig. 4). Similar results were observed with multiple cancer cell lines (Supplementary Table 2). These results demonstrate that MEDI-573 effectively inhibits the binding of IGF-I or IGF-II to IGF-1R, and subsequently inhibits the IGF-activated downstream signaling pathways and cell proliferation without inhibiting insulin-IR interaction.

Expression of IR-A versus IR-B in cancer cell lines

Increased expression of IR-A and IGF-II is reported in certain types of cancer and is proposed as a compensatory survival mechanism in cancer cells wherein IGF-1R signaling is inhibited (5, 11–17, 19, 20), which supports the rationale for IGF ligand neutralization. The relative abundance of IR-A versus IR-B mRNA was determined in multiple cancer cell lines using quantitative RT-PCR (5). The results show that at mRNA level, IR-A is the dominant isoform in these cancer cells, whereas IR-B is the dominant isoform in the normal liver of cynomolgus monkeys (Table 2).

MEDI-573 inhibits IGF-II activation of IR-A

MEDI-573 blocked IGF-II–stimulated (at 75 ng/mL) phosphorylation of IR-A and the downstream signal protein IRS-1 in two IR-A overexpressing cell lines: R-/IRA C9 cells (Fig. 2A and B) and MDA-MB-157 breast cancer cells (Fig. 2C and D). MDA-MB-157 cells primarily express the IR-A isoform (Table 2). In contrast, an IGF-1R–specific antibody did not block IGF-II–induced IR-A signaling pathway in either cell line.

Published OnlineFirst January 18, 2011; DOI: 10.1158/0008-5472.CAN-10-2274

Q2

Table 1. Summary of MEDI-573 characteristics

Antibody type	IgG2λ
Target	Human IGF-I and IGF-II
Binding affinity for hIGF-I	K_D = 294 pmol/L
Binding affinity for hIGF-II	K_D = 2 pmol/L
Binding affinity for mIGF-I	K_D = 2,000 pmol/L
Binding affinity for mIGF-II	K_D = 4 pmol/L
Binding to IGF-IGFBP3 complex	No significant binding detected (K_D > 1 μmol/L)
Binding to insulin	No significant binding detected (up to 0.2 μmol/L in BIAcore and 1 μmol/L in IR phosphorylation assay)

MEDI-573 inhibits IGF-II–stimulated cell proliferation in homogeneous and heterogeneous populations expressing either or both IGF-1R and IR-A

In *in vitro* cell proliferation assays, MEDI-573 inhibited IGF-II–stimulated proliferation of R-/IRA C9 cells (IC_{50} = 1.9 nmol/L; Fig. 3D), similar to its activity in NIH/IGF-1R cells (Fig. 3A). MEDI-573 displayed potent inhibition of proliferation in mixed cell populations of NIH/IGF-1R and R-/IRA C9 at different ratios, with similar IC_{50} values irrespective of the percentage of the IGF-1R–expressing versus the IR-A–expressing cells (Fig. 3A–D). In contrast, an IGF-1R–specific antibody showed the greatest inhibition of proliferation against pure populations of NIH/IGF-1R cells, but had only marginal activity when the heterogeneous cell population contained 25% R-/IRA C9 cells, and lost activity entirely when 50% or more of the heterogeneous cell population was R-/IRA C9 cells. Therefore, in cancers with both IR-A–expressing and IGF-1R–expressing cells, MEDI-573 may have greater and more consistent inhibition of cell proliferation than IGF-1R–targeting antibodies.

MEDI-573 inhibits the *in vivo* growth of xenograft models overexpressing IGF-1R and IGF

The antitumor activity of MEDI-573 was investigated in C32 cells (overexpress human IGF-II and human IGF-1R) and P12 cells (overexpress human IGF-I and human IGF-1R) when grown as xenografts in nude mice. MEDI-573 was highly active against the C32 model when administered as a single agent, producing dose-dependent *in vivo* TGI. Treatment with 30 or 60 mg/kg of MEDI-573 resulted in 86% and 91% TGI, respectively (Fig. 4A). A dose response was observed between the dose levels of 3 to 30 mg/kg ranging from 18% to 86% TGI. Similarly, MEDI-573 significantly inhibited the growth of P12

Table 2. Relative abundance of IR-A versus IR-B mRNA in normal and cancer cell lines

Cell lines	Cancer type	IR-A, %	IR-B, %
Normal cyno liver	Normal liver	<5	>95
Hep3B	Hepatocellular carcinoma	73	27
PLC	Hepatocellular carcinoma	52	48
HepG2	Hepatocellular carcinoma	77	23
MCF-7	Breast	60	40
MDA-MB157	Breast	>95	<5
BT-474	Breast	59	41
KPL-4	Breast	39	61
BT-20	Breast	60	40
BT-483	Breast	87	13
BT549	Breast	>95	<5
MDA-MB231-NIH	Breast	48	52
MDA-MB-231-KC	Breast	90	10
MDA-MB-468	Breast	50	50
5637	Bladder	53	47
HT-1197	Bladder	49	51
J82	Bladder	65	35
T24	Bladder	70	30
TCC-SUP	Bladder	53	47
UM-UC-3	Bladder	69	31
Lovo	Colorectal	67	33
A549	Lung	50	50
PC3	Prostate	48	51
R-/IRA C9[a]	Mouse fibroblast	100	0

[a]R-/IRA C9 is a mouse fibroblast cell line that does not express the mouse IGF-1R protein but was engineered to overexpress human IR-A. It is used as a control for IRA mRNA quantitative PCR.

Published OnlineFirst January 18, 2011; DOI: 10.1158/0008-5472.CAN-10-2274

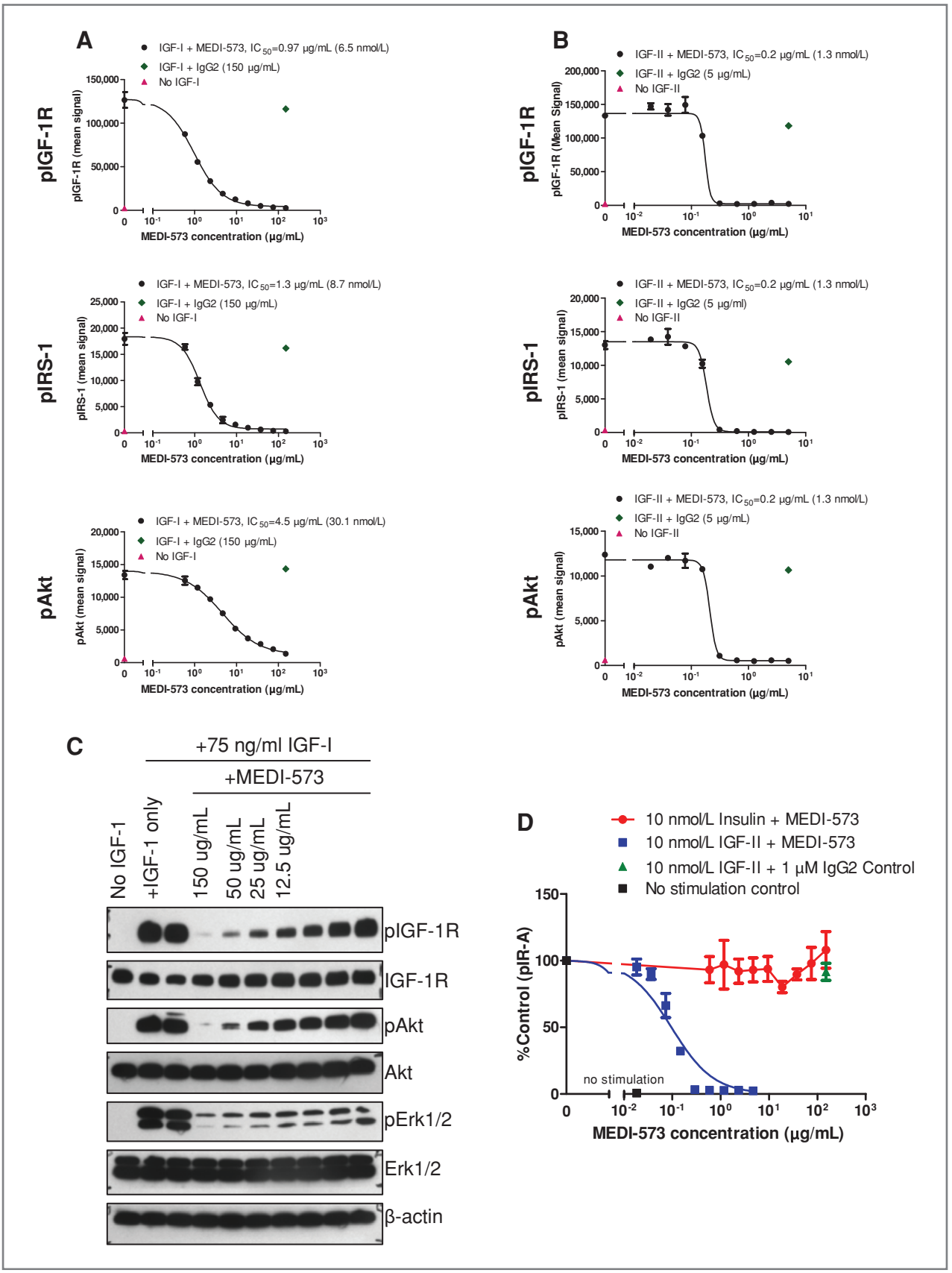

Published OnlineFirst January 18, 2011; DOI: 10.1158/0008-5472.CAN-10-2274

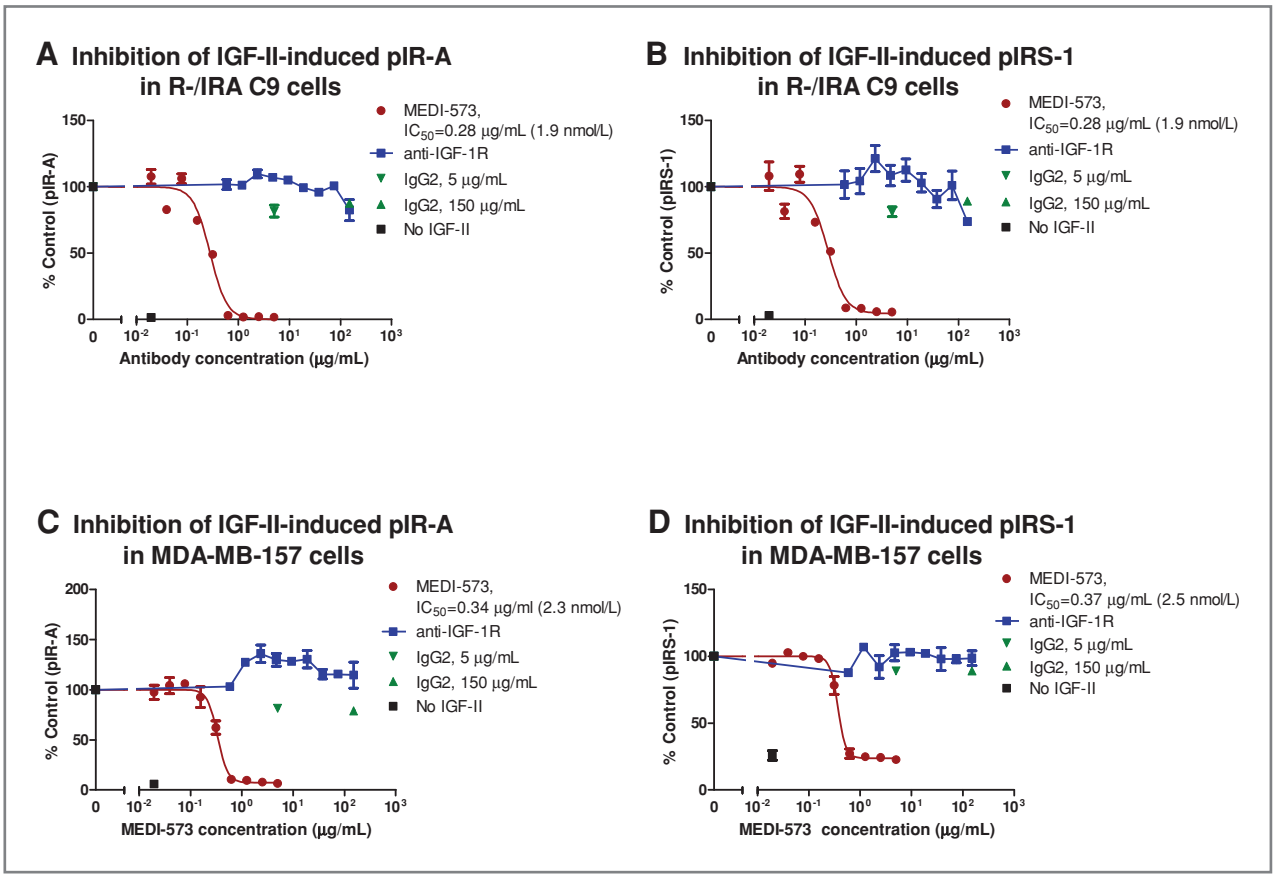

Figure 2. MEDI-573 inhibits IGF-II–induced phosphorylation of IR-A and IRS-1. MSD analysis of lysates from serum-starved R-/IRA C9 cells (A and B) or MDA-MB-157 cells (C and D) stimulated with 75 ng/mL IGF-II premixed with increasing concentrations of MEDI-573 (red, 0–5 μg/mL), or an IGF-1R–specific antibody (blue, 0–150 μg/mL), or an isotype control antibody (green, at 5 and 150 μg/mL). The levels of pIR-A (A, C) and pIRS-1 (B, D) are expressed on the *Y* axis as the percentage of the phosphorylation observed in positive control samples treated with IGF-II only.

tumors. A clear dose response was observed between the dose levels of 3 to 30 mg/kg in which, 3, 10, and 30 mg/kg resulted in TGI of 20%, 66%, and 86%, respectively. When MEDI-573 was administered at 60 mg/kg, the resulting TGI was similar to that of 30 mg/kg (Fig. 4B).

Modulation of pIGF-1R in P12 and C32 tumors was also examined 24 or 72 hours after the last dose. As seen in Figure 4C and D, there is a direct correlation between MEDI-573 dose and the decrease of tumor pIGF-1R levels, which in turn correlates with *in vivo* TGI (Fig. 4A and B). The serum concentrations of MEDI-573 from the animals were also determined in C32 tumors (data not shown) showing a strong correlation between increased serum concentrations of MEDI-573 and decreased levels of pIGF-1R.

^{18}F-FDG-PET imaging as a pharmacodynamic marker for MEDI-573 *in vivo* activity

The use of ^{18}F-FDG-PET imaging was investigated as a noninvasive pharmacodynamic readout for evaluating MEDI-573 *in vivo* activity using the P12 tumors, which respond to MEDI-573 with maximum TGI of more than 85% at doses of 30 mg/kg or greater after 2 weeks (4 doses; Fig. 4B). The effect of a single dose (40 mg/kg) of MEDI-573 on the uptake of ^{18}F-FDG in P12 tumors 1 day (day 2) or 3 days (day 4) after admin-

Figure 1. MEDI-573 inhibits IGF-induced phosphorylation of IGF-1R, IR-A, IRS-1, Akt, and Erk. A and B, MSD analysis of pIGF-1R (top), pIRS-1 (middle), and pAkt (bottom) levels from lysates of serum-starved NIH/IGF-1R cells treated (15 minutes) with IGF-I (75 ng/mL = 10 nmol/L; A) or IGF-II (75 ng/mL = 10 nmol/L; B) premixed with increasing concentration of MEDI-573 (0–150 μg/mL for IGF-I in A; 0–5 μg/mL for IGF-II in B) or an IgG2 isotype control antibody (green, 150 μg/mL in A; 5 μg/mL in B). C, immunoblots of lysates from serum-starved NIH/IGF-1R cells treated (15 minutes) with 75 ng/mL of IGF-I premixed with different concentrations of MEDI-573 (0 to 150 μg/mL) or 150 μg/mL of the IgG2 isotype control antibody. D, MSD analysis of pIR-A levels from the lysates of serum-starved R-/IRA C9 cells treated with IGF-II (blue, 75 ng/mL) or insulin (red, 58 ng/mL = 10 nmol/L) premixed with increasing concentrations of MEDI-573 (0–150 μg/mL) or an IgG2 isotype control antibody (green, 150 μg/mL = 1 μmol/L). Values are expressed as the percentage of the pIR-A levels of the respective positive controls, which are samples treated with IGF-II only for all IGF-II–stimulated samples (blue), or insulin only for all insulin-stimulated samples (red).

Published OnlineFirst January 18, 2011; DOI: 10.1158/0008-5472.CAN-10-2274

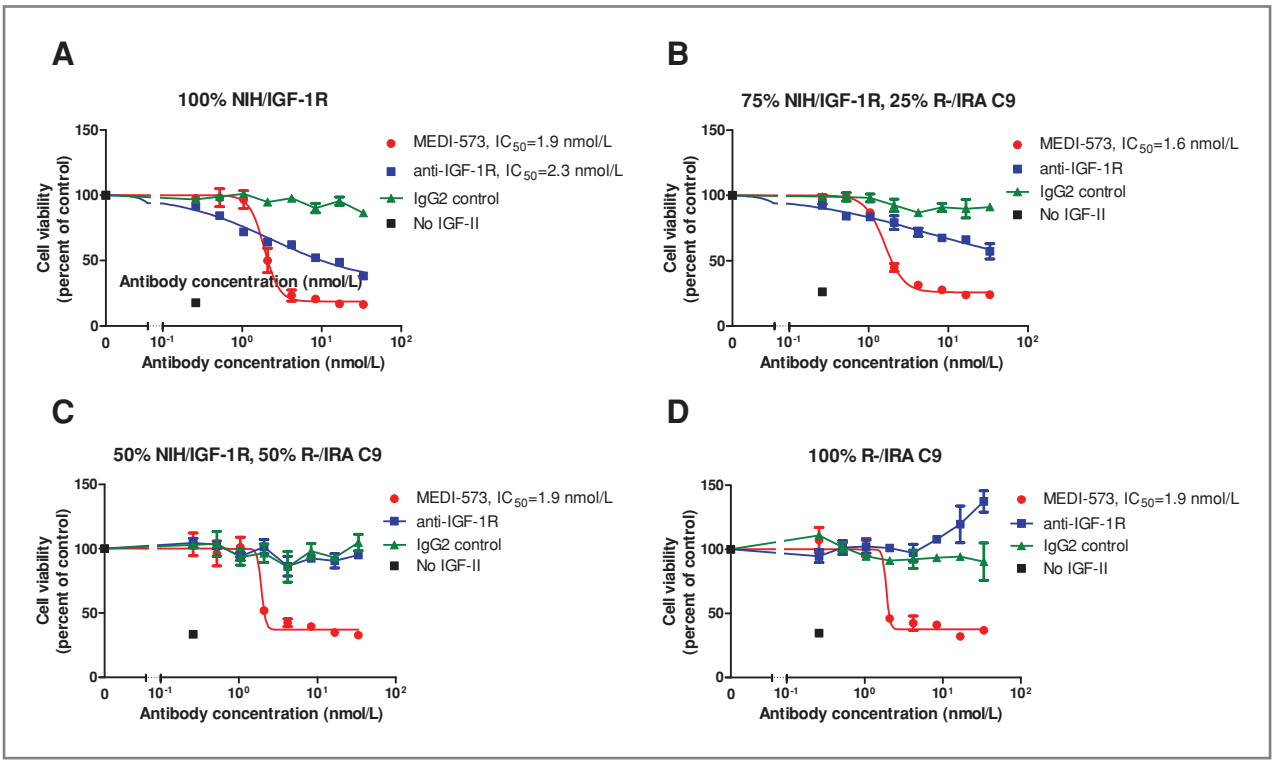

Figure 3. MEDI-573 inhibits IGF-II–stimulated proliferation of IGF-1R–overexpressing and IR-A–overexpressing cells in both heterogeneous and homogeneous populations with consistent activity. NIH/IGF-1R and R-/IRA C9 cells were seeded as 100% NIH/IGF-1R (A), a mixture of 75% NIH/IGF-1R and 25% R-IRA C9 (B), 50% each of NIH/IGF-1R and R-/IRA C9 (C), or a pure population of R-/IRA C9 (D). Cells were stimulated with 40 ng/mL of IGF-II and increasing concentrations (0–5 μg/mL) of MEDI-573 (red), or an IGF-1R–specific antibody (blue), or an IgG2 isotype control antibody (green). Numbers of viable cells were determined 3 days later using Cell Titer Glo and expressed as the percentage of positive control (stimulated with IGF-II only, no antibody) on the *Y* axis.

istration of MEDI-573 was determined. Tumor volumes were also measured.

On day 2, there was no significant change in tumor uptake of ^{18}F-FDG, reflected in MaxSUV, compared with day 0 (1 day before administration of MEDI-573) in the vehicle-treated group (Fig. 5A and D). In contrast, in the group dosed with 40 mg/kg of MEDI-573, all mice showed significant (P = 0.0002) decrease of MaxSUV (mean = 46%; Fig. 5A and D). There was also a significant (P = 0.0007) decrease (mean = 43%) in MaxSUV in the MEDI-573–treated group compared with the vehicle-treated group at day 2. The TGI in the MEDI-573 group compared with the vehicle group is not yet significant at day 2. There was an increase in tumor size from day 0 to 2 in both the vehicle-treated (average 507-mm^3 increase in tumor size, P = 0.0024) and the MEDI-573–treated group (296 mm^3, P = 0.019). The results demonstrated that reduction in ^{18}F-FDG uptake in P12 tumors can be detected as early as 24 hours after the first dose of MEDI-573, before significant TGI is observed.

When imaging was performed on day 4, there was an increase (23%, P = 0.0007) in MaxSUV compared with day 0 in the vehicle-treated group (Fig. 5B and D). In contrast, in the MEDI-573–treated group, 7 of 8 of the mice showed a decrease in MaxSUV at day 4 (29%, P = 0.0179; Fig. 5B and D). There was also a decrease in MaxSUV in the MEDI-573–treated group compared with vehicle-treated group at day 4 (47%, P = 0.0013). In addition, there was an increase in tumor size in the vehicle-treated group (increase of 418 mm^3, P = 0.0066) and a slight reduction in tumor size in the MEDI-573–treated group (68 mm^3, not significant) from days 0 to 4 (Fig. 5C). The MEDI-573–treated group showed a significant 52% TGI (P = 0.00376) compared with the vehicle-treated group at day 4.

^{18}F-FDG-PET imaging showed a reduction of ^{18}F-FDG uptake as early as 24 hours, and up to 72 hours, after the first dose of MEDI-573 in P12 tumors, consistent with the *in vivo* TGI activity of MEDI-573 in this model that was significant at 72 hours. Coupled with the greater than 85% TGI by 2 weeks achieved at doses of 30 mg/kg or greater in the P12 model, the reduction of ^{18}F-FDG uptake in the MEDI-573 groups, but not the vehicle groups, is consistent with the predicted *in vivo* activity of MEDI-573 in the P12 tumors.

Discussion

IGF signaling pathways are important in the development and progression of many solid tumors (1, 3, 4, 22, 24). As such, multiple IGF-1R inhibitors are being evaluated in various phases of clinical development in different tumor types (25, 26). There are some promising results in early clinical trials, particularly in patients with Ewing's sarcoma where complete

Published OnlineFirst January 18, 2011; DOI: 10.1158/0008-5472.CAN-10-2274

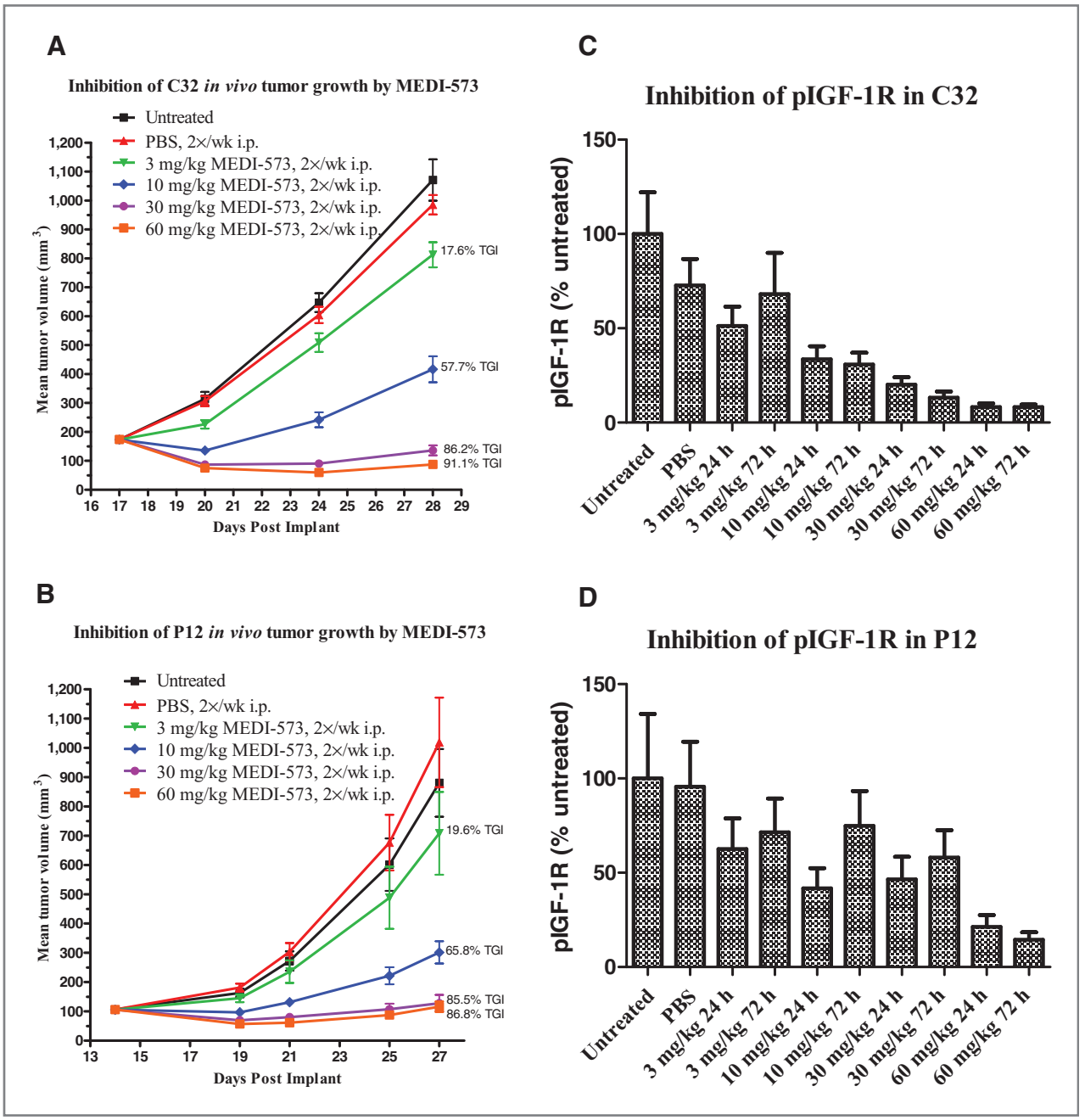

Figure 4. MEDI-573 inhibits *in vivo* growth of P12 and C32 xenograft tumors. A, C32 tumor volumes (mm^3) in nude mice dosed with MEDI-573 at 3, 10, 30, and 60 mg/kg, twice per week for 2 weeks. B, P12 tumor volumes (mm^3) in nude mice dosed with MEDI-573 at 3, 10, 30, and 60 mg/kg, twice per week for 2 weeks. C, MSD analysis of pIGF-1R levels in extracts of C32 tumor dosed with MEDI-573. D, MSD analysis of pIGF-1R levels in extracts of P12 tumor dosed with MEDI-573. pIGF-1R levels are expressed as the percentage of the levels from untreated tumors.

responses have been reported (38). The majority of IGF-targeting antibody therapies are IGF-1R–specific antibodies that inhibit the IGF-1R signaling pathway and may partially inhibit IR-A activity by disrupting the IR-A/IGF-1R hybrid receptors, but do not inhibit IR-A homodimers (28, 29). Because of the high degree of homology in the kinase domain, small-molecule kinase inhibitors which target IGF-1R will also inhibit IR-A and IR-B, which is crucial for glucose metabolism (25, 39). In comparison, disruption of IGF signaling pathways by neutralizing both IGF-I and IGF-II ligands (as does MEDI-573) offers the potential to broadly suppress the IGF system through the inhibition of both the IGF-1R and the IR-A receptors without interfering with glucose metabolism mediated by insulin/IR interaction.

To selectively target the IGF ligands, MEDI-573, a fully human IgG2 monoclonal antibody that neutralizes both

Published OnlineFirst January 18, 2011; DOI: 10.1158/0008-5472.CAN-10-2274

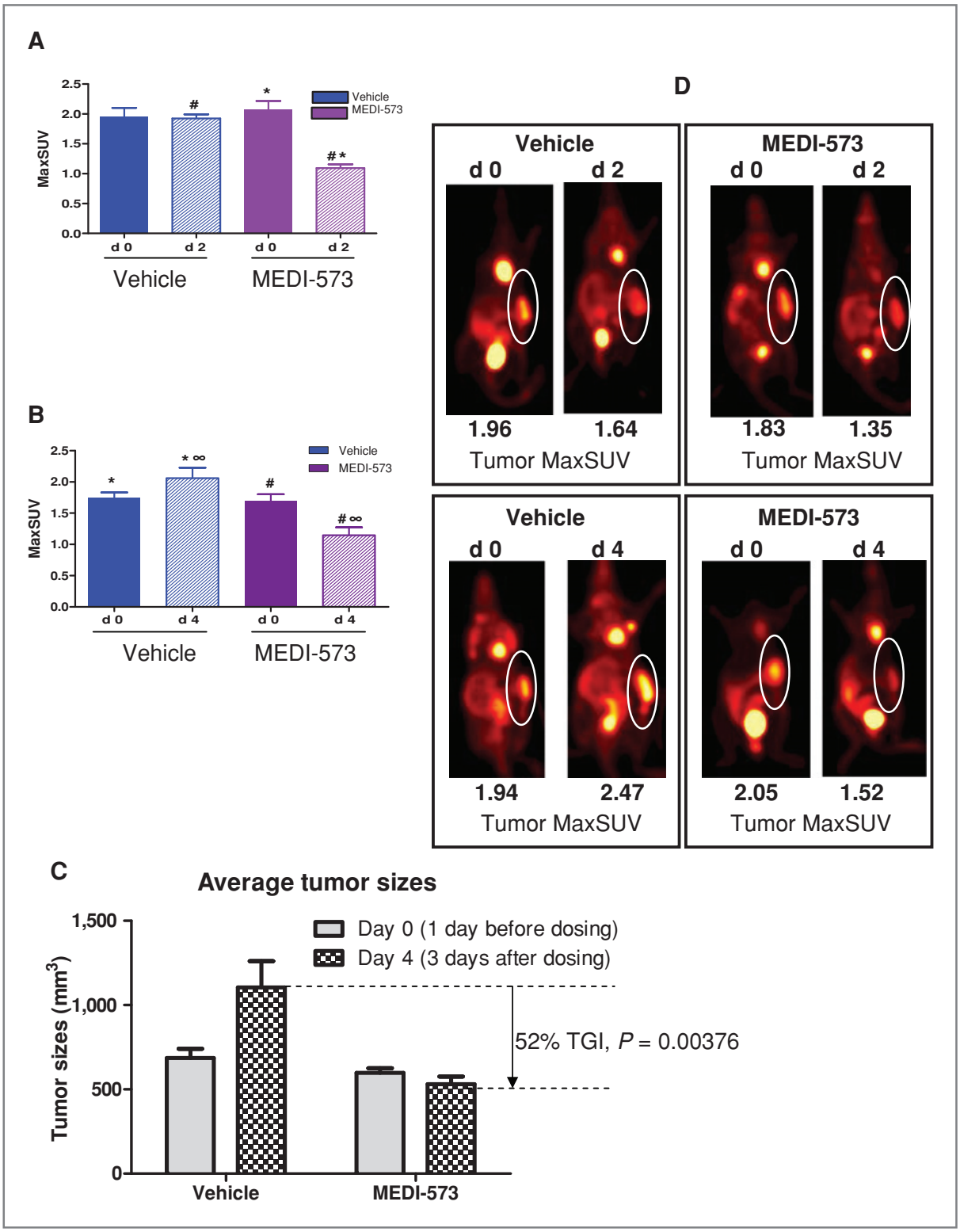

Figure 5. FDG-PET imaging as pharmacodynamic read-out for MEDI-573 *in vivo* activity in P12 tumors. The effect of a single dose (40 mg/kg) of MEDI-573 on the uptake of ^{18}F-FDG (reflected in MaxSUV on *Y* axis) in P12 tumors 1 day (day 2) or 3 days (day 4) after administration was determined. A, MaxSUV of tumor ^{18}F-FDG uptake at day 2 versus day 0. *, $P = 0.0002$ versus MEDI-573 day 0; #, $P = 0.0007$ versus vehicle day 2. B, MaxSUV of tumor ^{18}F-FDG uptake at day 4 versus day 0. *, $P = 0.0007$; #, $P = 0.0179$; and ∞, $P = 0.0013$. C, P12 tumor volumes (mm^3) at day 0 and day 4. D, single-slice ^{18}F-FDG-PET image of P12 xenograft-bearing nude mice.

Published OnlineFirst January 18, 2011; DOI: 10.1158/0008-5472.CAN-10-2274

IGF-I and IGF-II, was developed. MEDI-573 inhibits the IGF-induced activation of both the IGF-1R and the IR-A signaling pathways. MEDI-573 binds to IGF-I and IGF-II without cross-reactivity to human insulin and inhibits the IGF-induced phosphorylation of IGF-1R, IR-A, IRS-1, Akt, and Erk1/2 in IGF-1R–expressing or IR-A–expressing cell lines. In turn, this antibody blocks IGF-stimulated proliferation of cell lines expressing IGF-1R or IR-A. MEDI-573 inhibits the *in vivo* growth of MEF tumors that are dependent on autocrine IGF stimulation. Pharmacodynamic analysis of the pIGF-1R levels in tumor extracts from these *in vivo* studies showed dose-dependent inhibition of pIGF-1R by MEDI-573, and therefore confirmed *in vivo* that MEDI-573 directly inhibits the IGF signaling pathways. In comparison, human xenograft tumors that are not strongly driven by autocrine production of IGF showed only modest response to MEDI-573 in mouse models, due to the low cross-reactivity of MEDI-573 to mouse IGF-I. Mouse IGF-I has nearly equivalent biological activity to human IGF-I with respect to the activation of human IGF-1R (data not shown), which is not inhibited by MEDI-573. Xenograft models expressing receptors only (IGF-1R and/or IR-A) do not respond to MEDI-573 in mouse. Xenograft models expressing both IGF and the receptors have minor responses to MEDI-573 (data not shown). In contrast, in mouse models, IGF-1R–specific antibodies block the activation of tumor IGF-1R from both autocrine (human IGF) and paracrine (mouse IGF-I) IGF. Subsequently, IGF-1R–specific antibodies show better TGI activity compared with MEDI-573 in mouse. Therefore, human xenografts in mouse models are not suitable for testing the antitumor activity of MEDI-573.

The insulin receptor exists in 2 isoforms, IR-A and IR-B. IGF-II has significant affinity for IR-A, in addition to its affinity to IGF-1R. Recently, the role of IGF-II in regulating the IR-A pathway and cancer progression has been investigated. Overexpression of IGF-II and IR-A in breast cancer is well documented (5, 9, 40–46). We have also shown in a number of human cancer cell lines that IR-A is the dominant isoform expressed at mRNA level. MEDI-573 effectively inhibits IGF-II–induced phosphorylation of IR-A, IRS-1, and proliferation of IR-A–overexpressing cells as effectively as it inhibits the IGF-1R–overexpressing cells and mixed cell populations with various ratios of IR-A–expressing and IGF-1R–expressing cells. In contrast, an IGF-1R–specific antibody lost activity quickly when the heterogeneous cell population contained increasing percentages (25%–50%) of IR-A–expressing cells. MEDI-573 should have greater antitumor activity than IGF-1R antibodies in tumors that express both IGF-1R and IR-A, or IR-A alone (Fig. 3).

Epitope mapping studies indicated that MEDI-573 binds to the epitope that overlaps with F23 and F25, which are essential for binding to IGF-1R (36) and IGFBPs (37). BIAcore analysis confirmed that MEDI-573 does not bind to IGF-I/IGFBP3 or IGF-II/IGFBP3 complexes (data not shown) indicating that MEDI-573 preferentially binds to free IGF. Therefore, the majority of circulating IGF-I and IGF-II, which are bound to IGFBPs, should not act as a sink to deplete active MEDI-573 *in vivo*.

The feasibility of ^{18}F-FDG-PET imaging was demonstrated as a potential noninvasive pharmacodynamic readout for the *in vivo* activity of MEDI-573. Significant reduction of ^{18}F-FDG uptake in P12 tumors treated with a single dose of MEDI-573 at 1 and 3 days posttreatment was seen compared with either no changes or an increase of ^{18}F-FDG uptake in vehicle-treated groups at the same time points, respectively. At 3 days posttreatment, the reduction of ^{18}F-FDG uptake correlated with more than 50% TGI in the MEDI-573–treated group compared with the vehicle-treated group. Although the inhibition of tumor growth was not yet apparent at the 1-day time point, the reduction of ^{18}F-FDG uptake at this early time point correlated with the predicted TGI observed at later time points in this model. Thus, ^{18}F-FDG-PET imaging could provide a sensitive readout of MEDI-573 *in vivo* activity in clinical trials at early time points before responses could be detected in tumor sizes.

IGF ligand neutralization is a novel yet rational approach as targeted cancer therapy. There are published reports of IGF-neutralizing antibodies showing *in vivo* antitumor activity. Goya and colleagues (47) described a rat IgG2b antibody with neutralizing activity against both IGF-I and IGF-II that inhibited prostate cancer cell growth in human bone implanted in mice. Dransfield and colleagues (48) described an IGF-II-neutralizing human monoclonal antibody (DX-2647) that inhibited the growth of human hepatocarcinoma cells *in vitro* and slowed tumor growth *in vivo*. Interestingly, the *in vivo* activity of DX-2647 is moderate, slowing tumor growth instead of producing tumor stasis or regression, which is consistent with the hypothesis that the paracrine activation of the human IGF-1R by mouse IGF-I interferes with the *in vivo* activity of these IGF ligand antibodies in the mouse model.

Compared with reports of IGF-neutralizing antibodies, MEDI-573 is the only human monoclonal antibody that neutralizes both IGF-I and IGF-II without cross-reactivity to insulin, thus blocking the IGF-1R and IR-A signaling pathways and sparing the insulin/IR pathway. MEDI-573 should have greater activity as compared with an IGF-1R–specific antibody in tumors that express a mixture of IGF-1R and IR-A, or IR-A only. MEDI-573 is currently in phase 1 clinical trials for cancer patients with solid tumors.

Disclosure of Potential Conflicts of Interest

No potential conflicts of interest were disclosed.

Acknowledgments

We thank David Tonge for scientific input, Olivia Lecomte-Raeber (Abgenix), and Gadi Gazit-Bornstein (AstraZeneca/Abgenix) for antibody production and *in vitro* testing; Paul Kang (Amgen) and Ian Foltz (Amgen) for *in vivo* testing of the C32 model and scientific input; Scott Klakamp for BIAcore support; and Jaye Viner, Theresa LaVallee, Jiaqi Huang, Karen Mitz, and members of the MedImmune Product Development Team and Translational Science Sub-Team for insightful comments and reviewing the manuscript.

The costs of publication of this article were defrayed in part by the payment of page charges. This article must therefore be hereby marked *advertisement* in accordance with 18 U.S.C. Section 1734 solely to indicate this fact.

Received June 22, 2010; revised October 25, 2010; accepted November 24, 2010; published OnlineFirst January 18, 2011.

Published OnlineFirst January 18, 2011; DOI: 10.1158/0008-5472.CAN-10-2274

References

1. Pollak M. Insulin and insulin-like growth factor signalling in neoplasia. Nat Rev Cancer 2008;8:915–28.
2. De MP. Insulin and its receptor: structure, function and evolution. Bioessays 2004;26:1351–62.
3. Tao Y, Pinzi V, Bourhis J, Deutsch E. Mechanisms of disease: signaling of the insulin-like growth factor 1 receptor pathway–therapeutic perspectives in cancer. Nat Clin Pract Oncol 2007; 4:591–602.
4. Ryan PD, Goss PE. The emerging role of the insulin-like growth factor pathway as a therapeutic target in cancer. Oncologist 2008;13:16–24.
5. Sciacca L, Costantino A, Pandini G, Mineo R, Frasca F, Scalia P, et al. Insulin receptor activation by IGF-II in breast cancers: evidence for a new autocrine/paracrine mechanism. Oncogene 1999;18:2471–9.
6. Belfiore A, Frasca F, Pandini G, Sciacca L, Vigneri R. Insulin receptor isoforms and insulin receptor/insulin-like growth factor receptor hybrids in physiology and disease. Endocr Rev 2009;30:586–623.
7. Baserga R. The insulin receptor substrate-1: a biomarker for cancer?Exp Cell Res 2009;315:727–32.
8. Chitnis MM, Yuen JS, Protheroe AS, Pollak M, Macaulay VM. The type 1 insulin-like growth factor receptor pathway. Clin Cancer Res 2008;14:6364–70.
9. Frasca F, Pandini G, Scalia P, Sciacca L, Mineo R, Constantino A, et al. Insulin receptor isoform A, a newly recognized, high-affinity insulin-like growth factor II receptor in fetal and cancer cells. Mol Cell Biol 1999;19:3278–88.
10. Belfiore A. The role of insulin receptor isoforms and hybrid insulin/IGF-I receptors in human cancer. Curr Pharm Des 2007;13:671–86.
11. Belfiore A, Frasca F. IGF and insulin receptor signaling in breast cancer. J Mammary Gland Biol Neoplasia 2008;13:381–406.
12. Jones HE, Gee JM, Barrow D, Tonge D, Holloway B, Nicholson RI. Inhibition of insulin receptor isoform-A signalling restores sensitivity to gefitinib in previously de novo resistant colon cancer cells. Br J Cancer 2006;95:172–180.
13. Breuhahn K, Schirmacher P. Reactivation of the insulin-like growth factor-II signaling pathway in human hepatocellular carcinoma. World J Gastroenterol 2008;14:1690–8.
14. Avnet S, Sciacca L, Salerno M, Gancitano G, Cassarino MF, Longhi A, et al. Insulin receptor isoform A and insulin-like growth factor II as additional treatment targets in human osteosarcoma. Cancer Res 2009; 69:2443–52.
15. Sun Y, Gao D, Liu Y, et al. IGF2 is critical for tumorigenesis by synovial sarcoma oncoprotein SYT-SSX1. Oncogene 2006;25:1042–52.
16. Vella V, Pandini G, Sciacca L, Mineo R, Vigneri R, Pezzino V, et al. A novel autocrine loop involving IGF-II and the insulin receptor isoform-A stimulates growth of thyroid cancer. J Clin Endocrinol Metab 2002;87:245–54.
17. Chen YW, Boyartchuk V, Lewis BC. Differential roles of insulin-like growth factor receptor- and insulin receptor-mediated signaling in the phenotypes of hepatocellular carcinoma cells. Neoplasia 2009;11: 835–45.
18. Gallagher EM, O'Shea DM, Fitzpatrick P, Harrison M, Gilmartin B, Watson JA, et al. Recurrence of urothelial carcinoma of the bladder: a role for insulin-like growth factor-II loss of imprinting and cytoplasmic E-cadherin immunolocalization. Clin Cancer Res 2008; 14:6829–38.
19. Hendrickson AW, Haluska P. Resistance pathways relevant to insulin-like growth factor-1 receptor-targeted therapy. Curr Opin Investig Drugs 2009;10:1032–40.
20. Zhang H, Pelzer AM, Kiang DT, Yee D. Down-regulation of type I insulin-like growth factor receptor increases sensitivity of breast cancer cells to insulin. Cancer Res 2007;67:391–7.
21. Sachdev D, Yee D. Disrupting insulin-like growth factor signaling as a potential cancer therapy. Mol Cancer Ther 2007;6:1–12.
22. Baserga R. The insulin-like growth factor-I receptor as a target for cancer therapy. Expert Opin Ther Targets 2005;9:753–68.
23. Yuen JS, Macaulay VM. Targeting the type 1 insulin-like growth factor receptor as a treatment for cancer. Expert Opin Ther Targets 2008;12:589–603.
24. Frasca F, Pandini G, Sciacca L, Pezzino V, Squatrito S, Belfiore A, et al. The role of insulin receptors and IGF-I receptors in cancer and other diseases. Arch Physiol Biochem 2008;114:23–37.
25. Weroha SJ, Haluska P. IGF-1 receptor inhibitors in clinical trials–early lessons. J Mammary Gland Biol Neoplasia 2008;13:471–83.
26. Gualberto A, Pollak M. Clinical development of inhibitors of the insulin-like growth factor receptor in oncology. Curr Drug Targets 2009;10: 923–36.
27. Gualberto A, Karp DD. Development of the monoclonal antibody figitumumab, targeting the insulin-like growth factor-1 receptor, for the treatment of patients with non-small-cell lung cancer. Clin Lung Cancer 2009;10:273–80.
28. Gualberto A. Figitumumab (CP-751,871) for cancer therapy. Expert Opin Biol Ther 2010;10:575–85.
29. Wang Y, Hailey J, Williams D, Wang Y, Lipari P, Malkowski M, et al. Inhibition of insulin-like growth factor-I receptor (IGF-IR) signaling and tumor cell growth by a fully human neutralizing anti-IGF-IR antibody. Mol Cancer Ther 2005;4: 1214–21.
30. Pappano WN, Jung PM, Meulbroek JA, Wang YC, Hubbard RD, Zhang Q, et al. Reversal of oncogene transformation and suppression of tumor growth by the novel IGF1R kinase inhibitor A-928605. BMC Cancer 2009;9:314.
31. Wahner Hendrickson AE, Haluska P, Schneider PA, Loegering DA, Peterson KL, Attar R, et al. Expression of insulin receptor isoform A and insulin-like growth factor-1 receptor in human acute myelogenous leukemia: effect of the dual-receptor inhibitor BMS-536924 *in vitro*. Cancer Res 2009;69:7635–43.
32. Pietrzkowski Z, Sell C, Lammers R, Ullrich A, Baserga R. Roles of insulinlike growth factor 1 (IGF-1) and the IGF-1 receptor in epidermal growth factor-stimulated growth of 3T3 cells. Mol Cell Biol 1992;12: 3883–9.
33. Sell C, Rubini M, Rubin R, Liu JP, Efstratiadis A, Baserga R. Simian virus 40 large tumor antigen is unable to transform mouse embryonic fibroblasts lacking type 1 insulin-like growth factor receptor. Proc Natl Acad Sci USA 1993; 90:11217–21.
34. Myszka DG. Improving biosensor analysis. J Mol Recognit 1999; 12:279–84.
35. Gambhir SS. Quantitative assay development for PET. In: PET: Molecular Imaging and its Biological Applications, 125–216. Springer-Verlag New York, Inc. 2004.
36. Sara VR, Hall K. Insulin-like growth factors and their binding proteins. Physiol Rev 1990;70:591–614.
37. Carrick FE, Hinds MG, McNeil KA, Wallace JC, Forbes BE, Norton RS, Interaction of insulin-like growth factor (IGF)-I and -II with IGF binding protein-2: mapping the binding surfaces by nuclear magnetic resonance. J Mol Endocrinol 2005;34:685–98.
38. Olmos D, Postel-Vinay S, Molife LR, Okuno SH, Schuetze SM, Paccagnella ML, et al. Safety, pharmacokinetics, and preliminary activity of the anti-IGF-1R antibody figitumumab (CP-751,871) in patients with sarcoma and Ewing's sarcoma: a phase 1 expansion cohort study. Lancet Oncol 2010;11:129–35.
39. Haluska P, Carboni JM, Loegering DA, Lee FY, Wittman M, Saulnier MG, et al. *In vitro* and *in vivo* antitumor effects of the dual insulin-like growth factor-I/insulin receptor inhibitor, BMS-554417. Cancer Res 2006;66:362–71.
40. Vigneri P, Frasca F, Sciacca L, Pandini G, Vigneri R. Diabetes and cancer. Endocr Relat Cancer 2009;16:1103–23.
41. Frittitta L, Vigneri R, Stampfer MR, Goldfine ID. Insulin receptor overexpression in 184B5 human mammary epithelial cells induces a ligand-dependent transformed phenotype. J Cell Biochem 1995;57: 666–9.
42. Giorgino F, Belfiore A, Milazzo G, Costantino A, Maddux B, Whittaker J, et al. Overexpression of insulin receptors in fibroblast and ovary cells induces a ligand-mediated transformed phenotype. Mol Endocrinol 1991;5:452–9.
43. Gunter MJ, Hoover DR, Yu H, Wassertheil-Smoller S, Rohan TE, Manson JE, et al. Insulin, insulin-like growth factor-I, and risk of breast cancer in postmenopausal women. J Natl Cancer Inst 2009;101:48–60.

Published OnlineFirst January 18, 2011; DOI: 10.1158/0008-5472.CAN-10-2274

44. Mathieu MC, Clark GM, Allred DC, Goldfine ID, Vigneri R. Insulin receptor expression and clinical outcome in node-negative breast cancer. Proc Assoc Am Physicians 1997;109:565–71.

45. Pandini G, Vigneri R, Costantino A, Frasca F, Ippolito A, Fujita-Yamaguchi Y, et al. Insulin and insulin-like growth factor-I (IGF-I) receptor overexpression in breast cancers leads to insulin/IGF-I hybrid receptor overexpression: evidence for a second mechanism of IGF-I signaling. Clin Cancer Res 1999;5:1935–44.

46. Papa V, Pezzino V, Costantino A, Belfiore A, Giuffrida D, Frittitta L, et al. Elevated insulin receptor content in human breast cancer. J Clin Invest 1990;86:1503–10.

47. Goya M, Miyamoto S, Nagai K, Ohki Y, Nakamura K, Shitara K, et al. Growth inhibition of human prostate cancer cells in human adult bone implanted into nonobese diabetic/sever combined immunodeficient mice by a ligand-specific antibody to human insulin-like growth factors. Cancer Res 2004; 64:6252–58.

48. Dransfield DT, Cohen EH, Chang Q, Sparrow LG, Bentley JD, Dolezal O, et al. A human monoclonal antibody against insulin-like growth factor-II blocks the growth of human heptacellular carcinoma cell lines *in vitro* and *in vivo*. Mol Cancer Ther 2010;9: 1809–19.

Published OnlineFirst January 18, 2011; DOI: 10.1158/0008-5472.CAN-10-2274

Cancer Research
The Journal of Cancer Research (1916–1930) | The American Journal of Cancer (1931–1940)

AACR American Association for Cancer Research

Dual IGF-I/II–Neutralizing Antibody MEDI-573 Potently Inhibits IGF Signaling and Tumor Growth

Jin Gao, Jon W. Chesebrough, Susan A. Cartlidge, et al.

Cancer Res Published OnlineFirst January 18, 2011.